

Synthesis, molecular structures, and thermal decomposition of heterometallic (π -cyclooctadiene)platinum-bis(tricarbonyliron- μ_3 -chalcogenides)[Fe–Fe], (π -C₈H₁₂)Pt(μ_3 -X)₂Fe₂(CO)₆, where X = S, Se, or Te

A. A. Pasynskii,* N. I. Semenova, Yu. V. Torubaev, P. V. Belousov, K. A. Lyssenko, and Zh. V. Dobrokhotova

N. S. Kurnakov Institute of General and Inorganic Chemistry, Russian Academy of Sciences,
31 Leninsky prosp., 119991 Moscow, Russian Federation.
Fax: (095) 954 1279. E-mail: aapas@rambler.ru

Transmetallation of the Fe₃(μ_3 -X)₂(CO)₉ clusters (X = S, Se, or Te) under the action of (π -C₈H₁₂)PtCl₂ afforded new heterometallic clusters (π -C₈H₁₂)Pt(μ_3 -X)₂Fe₂(CO)₆ (**2–4**, respectively), which were characterized by X-ray diffraction analysis. The (π -C₈H₁₂)Pt fragment in these clusters is bound to two μ_3 -bridging chalcogen atoms X. The iron atoms are linked to each other. The coordination environment about the Pt atom is planar-square; the Pt...Fe distance is larger than 3.2 Å. In the synthesis of cluster **4**, a new Pt complex was also obtained for which the structure (CO)₂Pt(μ -Te)₂Pt(CO)₂ (**5**) was proposed. According to the results of differential scanning calorimetry, thermal decomposition of complex **5** gave rise only to PtTe, whereas complexes **1–4** gave products with the empirical formula Fe₂PtX₂C₂O₂. The influence of the steric effects on the geometry of the clusters is discussed.

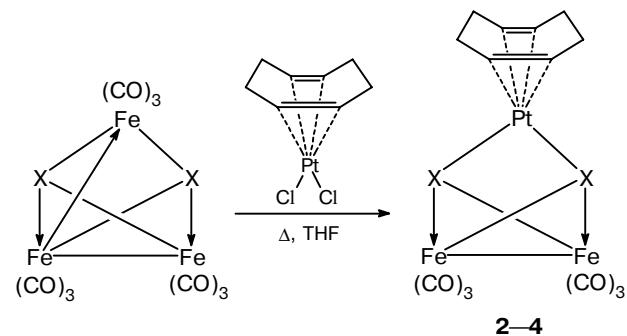
Key words: heterometallic clusters, π -complexes of platinum, iron carbonyl chalcogenides, cyclooctadiene, X-ray diffraction analysis, metal–metal bond, steric effects, thermal decomposition.

In the known (PPh₃)₂Pt(μ_3 -X)₂Fe₂(CO)₆ clusters, the Pt...Fe distances (3.302 and 3.410 Å in the case of X = S¹ and 3.459 and 3.589 Å in the case of X = Se²) are too large for the metal–metal bond to be formed, and the plane of the ligand environment about the platinum atom, which passes through the phosphorus and chalcogen atoms, is almost perpendicular to the Fe–Fe bond. Unlike these compounds, the (π -C₁₀H₁₂)Pt(μ_3 -S)₂Fe₂(CO)₆ cluster (**1**; π -C₁₀H₁₂ is dicyclopentadiene), which we have prepared recently, possesses one Fe–Pt bond (3.029 Å). As a result, the plane of the ligand environment about the platinum atom, which passes through the midpoints of the coordinated C=C bonds of the ligand and the sulfur atoms, deviates significantly from the perpendicular to the Fe–Fe bond.³ The repulsions between the dicyclopentadiene ligand and the carbonyl group at the iron atom (the C...C and C...O contacts in **1** are in the range of 3.5–3.8 Å)³ prevent more substantial shortening of the Fe–Pt bond. Apparently, the steric effects of repulsions between the ligands, which are to a large extent responsible for the possibility of heterometallic bonding, should depend substantially on the nature of the diene ligand at the platinum atom and the nature of the bridging chalcogen atoms whose covalent radii increase in the series S, Se, and Te (1.04, 1.17, and 1.37 Å, respectively).⁴ To verify this assumption, we synthesized the (π -cyclooctadiene)platinum-bis(tricarbonylironchalcogenide) clusters

(π -C₈H₁₂)Pt(X)₂Fe₂(CO)₆ (**2–4**) (X = S, Se, or Te) and established their structures.

Results and Discussion

By analogy with the synthesis of compound **1**, clusters **2–4** were prepared by transmetallation of the (μ_3 -X)₂Fe₃(CO)₉ clusters (X = S, Se, or Te) under the action of (π -C₈H₁₂)PtCl₂.



Complex **2** (X = S) was formed most readily. The preparation of complex **3** (X = Se) required more prolonged heating. The synthesis of complex **4** (X = Te) was accompanied by its gradual decomposition, which started before the initial (μ_3 -Te)₂Fe₃(CO)₉ cluster was completely consumed. As a result, a metal mirror was

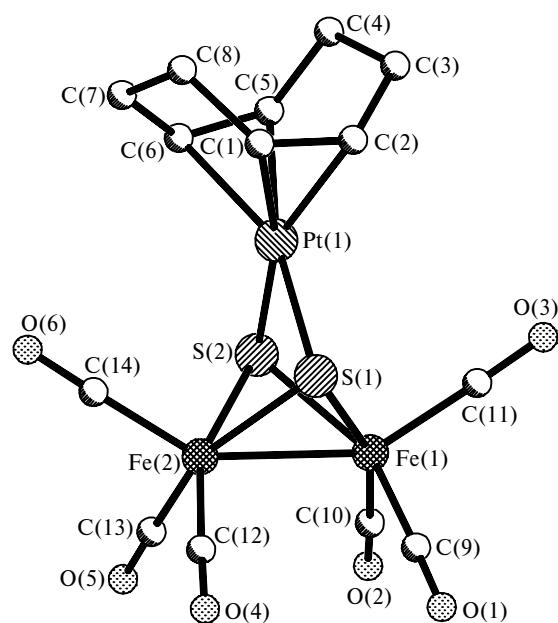


Fig. 1. Molecular structure of the $(\pi\text{-C}_8\text{H}_{12})\text{Pt}(\mu_3\text{-S})_2\text{Fe}_2(\text{CO})_6$ cluster (**2**).

formed on the walls of the reaction flask and a crimson-colored carbonylplatinum telluride complex appeared in the solution. According to the IR spectral data (ν_{CO} 2022 and 1965 cm^{-1}) and the results of thermal decomposi-

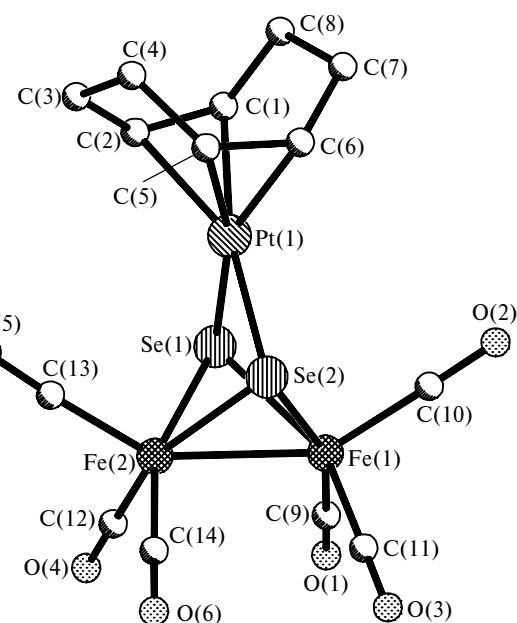


Fig. 2. Molecular structure of the $(\pi\text{-C}_8\text{H}_{12})\text{Pt}(\mu_3\text{-Se})_2\text{Fe}_2(\text{CO})_6$ cluster (**3**).

tion, the latter complex has the composition $(\text{CO})_4\text{Pt}_2\text{Te}_2$ (**5**) and is, apparently, a structural analog of the known binuclear $(\text{PPh}_3)_2\text{Pt}_2(\mu\text{-X})_2$ complexes.⁵ The possible scheme of formation of complex **5** may involve the stage

Table 1. Crystallographic data and details of X-ray diffraction study for complexes **2–4**

Parameter	2	3	4
Molecular formula	$\text{C}_{14}\text{H}_{12}\text{Fe}_2\text{O}_6\text{PtS}_2$	$\text{C}_{14}\text{H}_{12}\text{Fe}_2\text{O}_6\text{PtSe}_2$	$\text{C}_{14}\text{H}_{12}\text{Fe}_2\text{O}_6\text{PtTe}_2$
<i>M</i>	647.15	740.95	838.23
Diffractometer	SMART 1K CCD		Siemens P3/PC
Scan mode	ω scanning technique with a ω step of 0.3° frames were exposed for 10 s each		$\theta/2\theta$
<i>T</i> /K	110		298
Absorption correction	Empirical correction based on equivalent reflections		Azimuth ψ scanning technique
Space group	$P\bar{1}$	$P\bar{1}$	$P\bar{1}$
<i>a</i> /Å	7.575(1)	7.614(5)	7.818(2)
<i>b</i> /Å	11.260(2)	11.320(7)	10.507(2)
<i>c</i> /Å	11.274(2)	11.364(7)	12.255(3)
α /deg	113.286(4)	113.29(1)	103.05(3)
β /deg	100.208(4)	91.23(1)	97.57(3)
γ /deg	91.500(4)	99.52(1)	100.94(3)
<i>V</i>	864.3(2)	883.2(9)	946.7(3)
<i>Z</i>	2	2	2
<i>F</i> (000)	612	684	756
$\mu(\text{MoK}\alpha)/\text{cm}^{-1}$	99.98	136.70	119.28
<i>d</i> _{calc} /g cm ⁻³	2.487	2.786	2.940
$2\theta_{\text{max}}$ /deg	60	60	60
Number of measured reflections	9385	9983	5895
Number of independent reflections	4887 (<i>R</i> (int) = 0.0326)	4789 (<i>R</i> (int) = 0.0455)	5519 (<i>R</i> (int) = 0.0829)
<i>R</i> _w , calculated based on <i>F</i> ² based on all reflections	0.0957	0.1044	0.1433
<i>R</i> , calculated based on <i>F</i> based on reflections with <i>I</i> > $2\sigma(I)$	0.0393 (4222 refl.)	0.0415 (3755 refl.)	0.0530 (4408 refl.)
GOF	1.044	0.940	1.008

of additional transmetalation of **4** under the action of $(\pi\text{-C}_8\text{H}_{12})\text{PtCl}_2$ giving rise to the unstable intermediate $(\pi\text{-C}_8\text{H}_{12}\text{Pt})_2\text{Te}_2\text{Fe}(\text{CO})_3$. The latter compound underwent subsequent decomposition with elimination of metallic iron, whereas carbon oxide that formed in the course of the reaction replaced the cyclooctadiene ligands at the platinum atom.

The structures of clusters **2–4** were established by X-ray diffraction analysis (Figs. 1–3; Tables 1 and 2).

The results of X-ray diffraction study of compounds **2–4** not only confirmed their compositions and revealed the structural similarity of these clusters and compound **1** but also demonstrated that the geometry of these compounds is influenced in a complex way by steric effects of ligand–ligand repulsions, which depend on the nature both of the bridging chalcogen atoms and the organic ligand at the platinum atom. It should be noted that all four complexes **1–4** are isoelectronic, and

weak intermolecular interactions observed in the crystals exert an effect only on the molecular packing. In clusters **2–4**, the expected elongation of the Fe–Fe bond is observed (2.506, 2.538, and 2.612 Å) as the covalent radius of the bridging chalcogen atom increases in the series S < Se < Te. Like in all known planar-square platinum complexes, the Pt atom has the 16-electron structure, its ability to take part in additional interactions with the lone electron pairs of the Fe atoms being retained due to the presence of the unoccupied orbital. It should be noted that the Pt...Fe distances in cyclooctadiene sulfide- or selenide-bridged complexes **2** and **3** are 3.226 and 3.345 or 3.379 and 3.521 Å, respectively. These distances are substantially larger than the length of the usual Pt–Fe bond (for example, 2.55 Å in $(\text{CO})_8\text{Fe}_2\text{Pt}(\pi\text{-C}_8\text{H}_{12})$)⁶ and are close to the distances found in the above-mentioned phosphine clusters $(\text{PPh}_3)_2\text{Pt}(\mu_3\text{-X})_2\text{Fe}_2(\text{CO})_6$.^{1,2} Apparently, the weakness

Table 2. Selected bond lengths (*d*) and bond angles (ω) in complexes **2–4**

Complex	Bond	<i>d</i> /Å	Angle	ω /deg
2	Pt(I)–C(6)	2.184(5)	S(I)–Pt(I)–S(2)	78.10(5)
	Pt(I)–C(2)	2.203(5)	S(2)–Fe(I)–S(I)	78.15(5)
	Pt(I)–C(I)	2.218(5)	S(2)–Fe(I)–Fe(2)	57.03(5)
	Pt(I)–C(5)	2.235(6)	S(I)–Fe(I)–Fe(2)	56.81(4)
	Pt(I)–S(1)	2.2885(14)	S(I)–Fe(2)–S(2)	77.97(5)
	Pt(I)–S(2)	2.2909(13)	S(I)–Fe(2)–Fe(I)	56.87(4)
	Fe(I)–S(2)	2.2846(16)	S(2)–Fe(2)–Fe(I)	56.62(4)
	Fe(I)–S(I)	2.2921(15)	Pt(I)–S(I)–Fe(2)	89.59(5)
	Fe(I)–Fe(2)	2.5064(12)	Pt(I)–S(I)–Fe(I)	93.84(5)
	Fe(2)–S(I)	2.2903(15)	Fe(2)–S(I)–Fe(I)	66.32(4)
	Fe(2)–S(2)	2.2953(17)	Fe(I)–S(2)–Pt(I)	93.97(5)
	C(1)–C(2)	1.388(9)	Fe(I)–S(2)–Fe(2)	66.36(5)
	C(5)–C(6)	1.382(9)	Pt(I)–S(2)–Fe(2)	89.40(5)
	Pt(I)–C(6)	2.189(6)	Se(I)–Fe(I)–Fe(2)	58.02(5)
	Pt(I)–C(I)	2.211(7)	Se(2)–Fe(I)–Fe(2)	57.97(4)
	Pt(I)–C(2)	2.213(6)	Se(2)–Fe(2)–Se(I)	78.55(4)
	Pt(I)–C(5)	2.230(6)	Se(2)–Fe(2)–Fe(I)	58.02(4)
3	Pt(I)–Se(I)	2.3983(13)	Se(I)–Fe(2)–Fe(I)	57.99(4)
	Pt(I)–Se(2)	2.4028(12)	Fe(I)–Se(I)–Fe(2)	63.99(4)
	Fe(I)–Se(I)	2.3945(16)	Fe(I)–Se(I)–Pt(I)	94.54(5)
	Fe(I)–Se(2)	2.3945(15)	Fe(2)–Se(I)–Pt(I)	89.65(5)
	Fe(I)–Fe(2)	2.5377(18)	Fe(2)–Se(2)–Fe(I)	64.02(4)
	Fe(2)–Se(2)	2.3932(15)	Fe(2)–Se(2)–Pt(I)	89.59(5)
	Fe(2)–Se(I)	2.3950(18)	Fe(I)–Se(2)–Pt(I)	94.42(6)
	C(1)–C(2)	1.359(11)		
	C(5)–C(6)	1.422(10)		
4	Pt(I)–C(6)	2.220(8)	Te(2)–Pt(I)–Te(I)	79.08(3)
	Pt(I)–C(5)	2.220(8)	Te(I)–Fe(I)–Te(2)	78.63(5)
	Pt(I)–C(2)	2.223(8)	Te(I)–Fe(I)–Fe(2)	58.95(5)
	Pt(I)–C(I)	2.244(9)	Te(2)–Fe(I)–Fe(2)	59.12(5)
	Pt(I)–Te(2)	2.5723(10)	Te(I)–Fe(2)–Te(2)	79.60(5)
	Pt(I)–Te(I)	2.5820(10)	Te(I)–Fe(2)–Fe(I)	60.07(4)
	Fe(I)–Te(I)	2.5889(15)	Te(2)–Fe(2)–Fe(I)	60.01(5)
	Fe(I)–Te(2)	2.5901(15)	Fe(2)–Te(I)–Pt(I)	99.53(5)
	Fe(I)–Fe(2)	2.6120(19)	Fe(2)–Te(I)–Fe(I)	60.97(5)
	Fe(2)–Te(I)	2.5592(15)	Pt(I)–Te(1)–Fe(I)	79.71(5)
	Fe(2)–Te(2)	2.5666(16)	Fe(2)–Te(2)–Pt(I)	99.59(4)
	C(1)–C(2)	1.434(15)	Fe(2)–Te(2)–Fe(I)	60.86(5)
	C(5)–C(6)	1.393(12)	Pt(I)–Te(2)–Fe(I)	79.87(4)

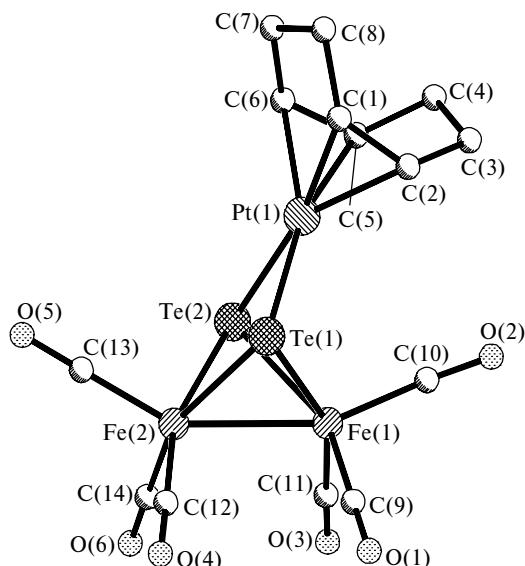


Fig. 3. Molecular structure of the $(\pi\text{-C}_8\text{H}_{12})\text{Pt}(\mu_3\text{-Te})_2\text{Fe}_2(\text{CO})_6$ cluster (**4**).

of Fe—Pt bonding results from steric repulsions between the $\pi\text{-C}_8\text{H}_{12}$ ligand and the carbonyl groups (the shortest C...C and C...O contacts between the ligands are approximately 3.8 Å), which prevent the Pt and Fe atoms from coming closer together. An analogous effect is observed in the $(\text{PPh}_3)_2\text{Pt}(\mu_3\text{-X})_2\text{Fe}_2(\text{CO})_6$ clusters in which the shortest C...C and C...O contacts are in the range of 3.5–3.8 Å^{1,2} due to repulsions between the phenyl groups of the triphenylphosphine ligands and the carbonyl groups.

The replacement of the selenium atoms in cluster **3** by the bulkier tellurium atoms (cluster **4**) causes the unexpected deviation of the plane of the ligand environment about the platinum atom, which passes through the midpoints of the double C=C bonds and the tellurium atoms, from the perpendicular to the Fe...Fe axis. This situation is analogous to that observed in dicyclopentadiene cluster **1**. However, the Fe—Pt bond in cluster **4** is substantially weaker (3.314 Å), whereas the second shortest Fe...Pt distance is increased to 3.921 Å. Nevertheless, the repulsions between the cyclooctadiene ligand and the carbonyl group in cluster **4** (the C...C and C...O contacts are in the range of 3.5–3.8 Å) prevent the Fe and Pt atoms from coming closer together.

The role of ligand—ligand repulsions in heterometallic bonding is confirmed by the geometry of dicyclopentadiene sulfide cluster **1** (Fig. 4). In this cluster, the rather short Pt—Fe bonding distance (3.029 Å) appears on the side of the unsymmetrical $\pi\text{-C}_{10}\text{H}_{12}$ ligand where the larger PtC₅ cavity is present (Fig. 4, *b*), *i.e.*, on the side where the repulsion between the diene ligand and CO at this Fe...Pt distance is weaker, rather than on the side of the PtC₄ cavity (Fig. 4, *a*) whose size is equal to those in cyclooctadiene clusters **2**–**4** (Fig. 4). In the nitrosyl cluster $(\text{PPh}_3)_2\text{Pt}(\mu_3\text{-S})_2\text{Fe}_2(\text{NO})_4$,⁷ which con-

tains only four NO groups instead of six CO groups present in the $(\text{PPh}_3)_2\text{Pt}(\mu_3\text{-S})_2\text{Fe}_2(\text{CO})_6$ cluster,¹ the steric effects of the ligand—ligand repulsions involving two bulky triphenylphosphine ligands are apparently less significant. As a result, the Pt and Fe atoms are located at the bonding Pt—Fe distances of 2.887(3) and 2.973(3) Å, the short contacts (3.3–3.8 Å) between the phenyl and nitrosyl groups (similar to those mentioned above for the phenyl and carbonyl groups) being retained (evidently, the role of the electronic differences between NO and CO must not be ruled out).

Experimental

All operations associated with the synthesis and isolation of the complexes were carried out under an atmosphere of argon and in anhydrous solvents. The $(\text{C}_8\text{H}_{12})\text{PtCl}_2$ and $\text{Fe}_3\text{X}_2(\text{CO})_9$ complexes, where X = S, Se, or Te, were prepared according to procedures described previously.^{8,9} The IR spectra were recorded on a Specord 75IR spectrophotometer in KBr pellets. Thermal decomposition of the complexes was studied by differential scanning calorimetry on a Mettler TA-4000 thermo-analyzer on heating of the specimens under an atmosphere of dry argon.

(π -Cyclooctadiene)platinum-bis(tricarbonyliron- μ_3 -sulfide)[Fe—Fe], $(\text{COD})\text{Pt}(\mu_3\text{-S})_2\text{Fe}_2(\text{CO})_6$ (2**).** The $\text{Fe}_3\text{S}_2(\text{CO})_9$ complex (0.52 g, 1.07 mmol) was added to a colorless solution of $(\text{C}_8\text{H}_{12})\text{PtCl}_2$ (0.4 g, 1.07 mmol) in THF (60 mL). The resulting dark-cherry solution was refluxed for 9 h. The red solution that formed was filtered off from the dark-brown precipitate (0.17 g) and the precipitate was washed with THF (10 mL). The combined solutions were concentrated to 1/4 of the initial volume and kept at -18 °C for 2 days. The red-orange crystalline product that precipitated was separated from the solution, washed with hexane, and dried. The yield was 0.24 g (35%). Found (%): C, 25.85; H, 2.65; S, 9.90. $\text{C}_{14}\text{H}_{12}\text{Fe}_2\text{O}_6\text{PtS}_2$. Calculated (%): C, 25.97; H, 1.87; S, 9.89. IR (KBr), ν/cm^{-1} : 550 s, 570 s, 610 m, 800 w, 820 w, 1940 s, 1955 s, 1975 s, 2000 s, 2052 m. Single crystals were used for X-ray diffraction analysis.

The quantitative elimination of the following fragments was demonstrated by differential scanning calorimetry:

C_8H_{12}	4 CO
Found (%)	16.7
Calculated (%)	16.0

The final decomposition product has the composition $\text{Fe}_2\text{PtS}_2\text{C}_2\text{O}_2$.

(π -Cyclooctadiene)platinum-bis(tricarbonyliron- μ_3 -selenide)[Fe—Fe], $(\text{COD})\text{Pt}(\mu_3\text{-Se})_2\text{Fe}_2(\text{CO})_6$ (3**).** The $\text{Fe}_3\text{Se}_2(\text{CO})_9$ complex (0.3 g, 0.53 mmol) was added to a colorless solution of $(\text{C}_8\text{H}_{12})\text{PtCl}_2$ (0.2 g, 0.53 mmol) in THF (40 mL). The resulting dark-cherry solution was refluxed for 23 h. The bright-red solution that formed was filtered off from the dark-brown precipitate (0.2 g) and the precipitate was washed with THF (10 mL). The combined solutions were concentrated to 1/4 of the initial volume and then hexane (2.5 mL) was added. The mixture was kept at -18 °C for 2 days. The red crystalline product that precipitated was separated from the solution, washed with hexane, and dried *in vacuo*. The yield was 0.1 g (25%). Found (%): C, 23.59. $\text{C}_{14}\text{H}_{12}\text{Fe}_2\text{O}_6\text{PtSe}_2$. Calculated (%): C, 22.69. IR (KBr), ν/cm^{-1} : 542 s, 565 s, 600 m, 1920 s, 1960 s, 1985 v.s., 2030 s. Single crystals were used for X-ray diffraction analysis.

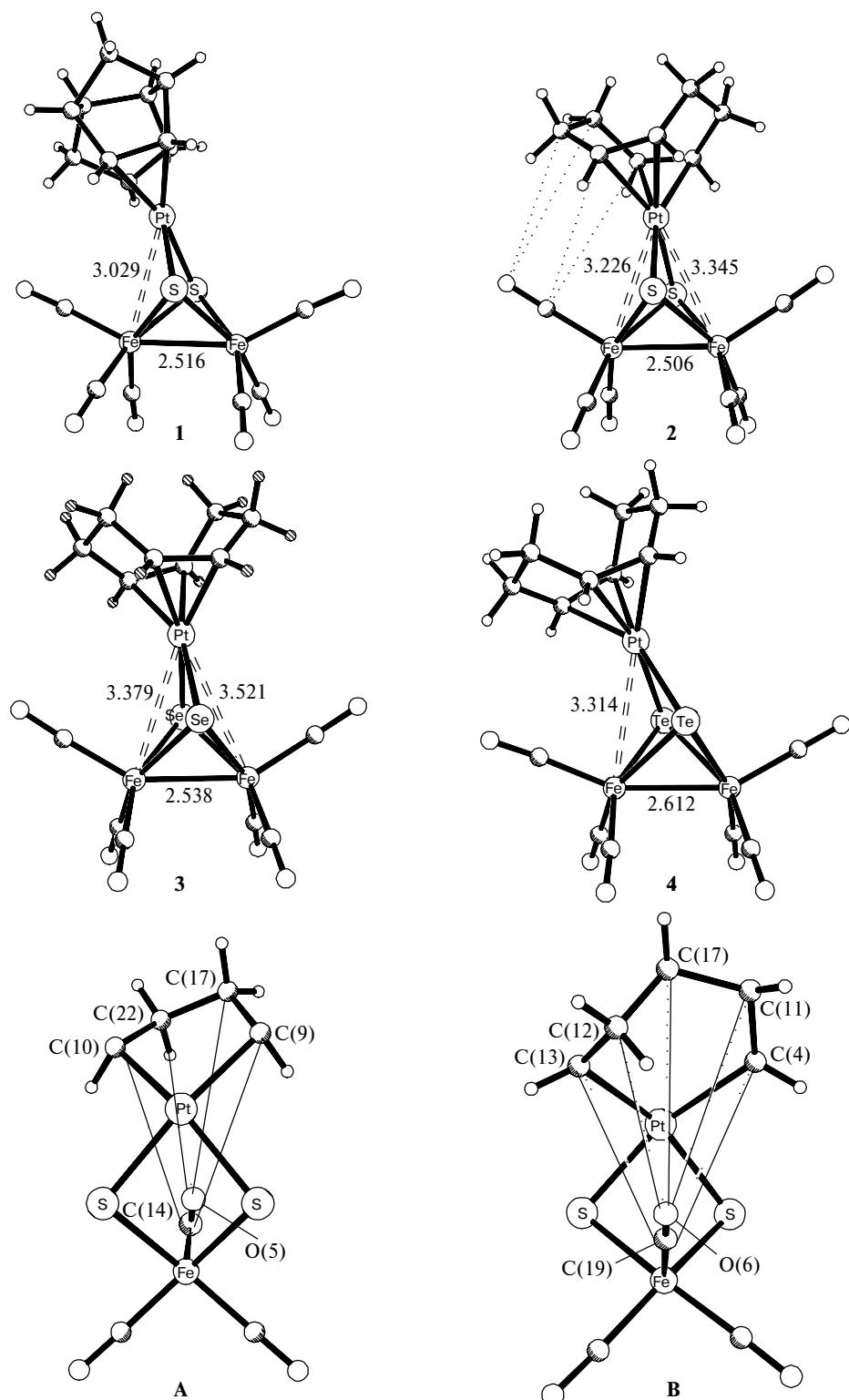


Fig. 4. The M–M bonds in clusters **1–4** and nonbonding ligand–ligand interactions in the clusters $(\pi\text{-C}_8\text{H}_{12})\text{Pt}(\mu_3\text{-S})_2\text{Fe}_2(\text{CO})_6$ (**A**) and $(\pi\text{-C}_{10}\text{H}_{12})\text{Pt}(\mu_3\text{-S})_2\text{Fe}_2(\text{CO})_6$ (**B**).

A				B			
Bond	$d/\text{\AA}$	Bond	$d/\text{\AA}$	Bond	$d/\text{\AA}$	Bond	$d/\text{\AA}$
C(14)–C(20)	5.157	O(5)–C(22)	3.851	O(6)–C(12)	3.477	C(19)–C(13)	3.659
C(14)–C(9)	4.386	O(5)–C(17)	4.546	O(6)–C(11)	4.646	C(19)–C(4)	4.038
						O(6)–C(17)	4.608

The quantitative elimination of the following fragments was demonstrated by differential scanning calorimetry:

	C ₈ H ₁₂	4 CO
Found (%)	14.6	15.1
Calculated (%)	14.5	13.8

The final decomposition product has the composition Fe₂PtSe₂C₂O₂.

(π -Cyclooctadiene)platinum-bis(tricarbonyliron- μ_3 -telluride)[Fe—Fe], (COD)Pt(μ_3 -Te)₂Fe₂(CO)₆ (4**), and tetracarbonyldiplatinum ditelluride, (CO)₄Pt₂Te₂ (**5**). The Fe₃Te₂(CO)₉ complex (0.36 g, 0.53 mmol) was added to a colorless solution of (C₈H₁₂)PtCl₂ (0.2 g, 0.53 mmol) in THF (40 mL). The resulting dark-violet solution was refluxed for 8 h (the course of the reaction was monitored by TLC) until the intensity of the orange spot of the reaction product began to decrease. A dark brown-crimson-colored solution and a black precipitate were obtained. The solution was concentrated and the solid precipitate was extracted with hexane (40 mL). The cherry solution was concentrated to 1/3 of the initial volume and kept at -18 °C for 1 day. The dark-violet (almost black) crystals of the initial complex Fe₃Te₂(CO)₉ (0.05 g) that precipitated were separated from the solution, washed with hexane, and dried. Subsequent extraction with CH₂Cl₂ (15 mL) afforded a dark orange-crimson-colored solution, which was concentrated to 1/3 of the initial volume. Then hexane (6 mL) was added and the reaction mixture was kept at -18 °C for 2 days. The red prismatic crystals of **4** that precipitated were separated from the solution, washed with hexane, and dried. The yield was 0.06 g (13.6% with respect to Te). Found (%): C, 19.90; H, 0.93. C₁₄H₁₂Fe₂O₆PtTe₂. Calculated (%): C, 20.06; H, 1.44.**

IR (KBr), v/cm⁻¹: 576 s, 608 s, 1925 s, 1970 s, 1980 s, 2025 s. Single crystals were used for X-ray diffraction analysis.

The quantitative elimination of the following fragments was demonstrated by differential scanning calorimetry:

	C ₈ H ₁₂	4 CO
Found (%)	12.9	13.3
Calculated (%)	12.5	12.8

The final decomposition product has the composition Fe₂PtTe₂C₂O₂.

Subsequent extraction of the resulting precipitate with hot CH₂Cl₂ (50 mL) afforded a crimson-colored solution, which was concentrated to 1/3 of the initial volume and kept at -18 °C for one day. The black-crimson-colored finely crystalline precipitate of complex **5** that formed was separated from the solution, washed with hexane, and dried. The yield was 0.02 g (5% with respect to Te). Found (differential scanning calorimetry) (%): CO 14.8. For C₄O₄Pt₂Te₂. Calculated (%): CO 15.0. The final decomposition product has the composition Pt₂Te₂. IR (KBr), v/cm⁻¹: 550 w, 582 s, 1920 s, 1965 s, 2022 s.

X-ray diffraction study of complexes **2–**4**.** The principal crystallographic data and the details of the refinement of complexes **2**–**4** are given in Table 1. The structures were solved by the direct method and refined by the full-matrix least-squares method in the anisotropic-isotropic approximation based on *F*². The positions of the H atoms were revealed from difference electron density syntheses and refined using the riding model. All calculations were carried out using the SHELXTL PLUS program package (version 5.0).¹⁰ The atomic coordinates and the thermal parameters were deposited with the Cambridge Structural Database. X-ray diffraction analysis was performed in the Center of X-ray Diffraction Studies (A. N. Nesmeyanov Institute of Organoelement Compounds of the Russian Academy of Sciences).

This work was financially supported by the Russian Foundation for Basic Research (Project Nos. 99-03-32806 and 00-03-32626).

References

1. A. A. Pasynskii, B. I. Kolobkov, S. E. Nefedov, I. L. Eremenko, E. S. Koltun, A. I. Yanovsky, and Yu. T. Struchkov, *J. Organomet. Chem.*, 1993, **454**, 22.
2. V. Day, D. A. Lesch, and T. B. Rauchfuss, *J. Am. Chem. Soc.*, 1982, **104**, 1290.
3. A. A. Pasynskii, N. I. Semenova, Yu. V. Torubaev, and K. A. Lyssenko, *Zh. Neorg. Khim.*, 2001, **46**, 1987 [*Russ. J. Inorg. Chem.*, 2001, **46** (Engl. Transl.)].
4. L. Pauling, *The Nature of the Chemical Bond*, University Press, Cornell, 1960.
5. C. E. Bryant, T. S. A. Hor, N. D. Nowells, and D. M. P. Mingos, *J. Chem. Soc., Chem. Commun.*, 1983, 1118.
6. L. S. Farrugia, J. A. K. Howard, P. Mitrprachahon, F. G. A. Stone, and P. Woodward, *J. Chem. Soc., Dalton Trans.*, 1981, 1134.
7. A. M. Mazani, J. P. Fackler, Jr., M. K. Gallagher, and D. Seyferth, *Inorg. Chem.*, 1983, **22**, 2593.
8. J. Chatt, L. M. Vallarino, and L. M. Venanzi, *J. Chem. Soc.*, 1957, 2496.
9. W. Hieber and J. Gruber, *Z. Anorg. Allgem. Chem.*, 1958, **B296**, 91.
10. G. M. Sheldrick, in *Crystallographic Computing 3: Data Collection, Structure Determination, Proteins and DataBases*, Clarendon Press, New York, 1985, 175.

Received July 18, 2001;
in revised form September 21, 2001